

A DESI DR1 Radial-Velocity Variability Search for Unseen Companions: Discovery of a Strong Compact-Object Candidate around an M0 Dwarf

Aiden Smith (A.I Sloperator)

January 15, 2026

Abstract

We present a conservative, fully reproducible search for radial-velocity (RV) variability in public DESI Data Release 1 (DR1) Milky Way Survey per-epoch spectra, targeting unseen companions to late-type stars. Starting from per-epoch RV measurements, we define a global variability significance and a leave-one-out robust statistic to identify systems whose RV variability cannot be explained by measurement noise alone. We then apply a “negative space” validation pipeline combining Gaia DR3 astrometry, LAMOST spectroscopy, WISE infrared photometry, GALEX ultraviolet imaging, TESS time-domain photometry, and Legacy Survey imaging to isolate systems that show strong gravitational effects but no detectable luminous companion.

The top candidate from this pipeline is Gaia DR3 3802130935635096832, a LAMOST-classified M0 dwarf with five public RV measurements (one from LAMOST DR7 and four from DESI DR1) spanning 5.9 years and a total RV range of 146.07 km s^{-1} . A hardened RV analysis yields a global significance of the variability of $S = 43.8$ and a leave-one-out robust significance of $S_{\text{robust}} = 33.1$, with one high-leverage DESI epoch explicitly vetted and found to be physically consistent and non-artifactual. Bayesian Keplerian modeling of the combined LAMOST+DESI RVs, assuming a $0.5 M_{\odot}$ M0 primary, gives a posterior median period of $P = 21.8$ days, semi-amplitude $K = 95 \text{ km s}^{-1}$, eccentricity $e = 0.18$, mass function $f(M) = 1.95 M_{\odot}$, and minimum companion mass $M_{2,\min} = 2.7 M_{\odot}$, with 68% credible interval $1.5\text{--}4.5 M_{\odot}$. The posterior probability that the unseen companion is more massive than $1.4 M_{\odot}$ is 87%, with a 37% probability that it exceeds $3 M_{\odot}$.

Spectrophotometric modeling of the LAMOST dM0 spectrum and Gaia photometry yields a distance of 495 ± 91 pc, while the Gaia parallax is essentially unconstraining and accompanied by significant astrometric excess noise and $\text{RUWE} = 1.95$, consistent with orbital photocenter wobble at the expected ~ 0.3 mas level. The system is deeply detached: the M0 primary fills only $\approx 5\%$ of its Roche lobe for the favored solution, naturally explaining the absence of ellipsoidal variability in the TESS light curve, which constrains periodic modulation in the relevant period range to below a few hundred parts per million. There is no infrared excess in WISE, no ultraviolet counterpart in GALEX, and the spectral energy distribution is consistent with a single M0 dwarf.

We therefore classify this object as a strong dark compact companion candidate, most likely hosting either a neutron star or a low-mass black hole, while acknowledging that a massive, cool white dwarf cannot yet be fully excluded. We make no claim of a definitive compact-object detection. All analysis scripts and intermediate products are released in an open GitHub repository, enabling full reproducibility and independent scrutiny of this candidate and of the general DESI DR1 unseen-companion search pipeline.

1 Introduction

Non-interacting compact remnants—white dwarfs (WDs), neutron stars (NSs), and black holes (BHs)—are expected to be numerous in the Milky Way, but are challenging to detect in the absence of accretion or other luminous signatures. Gravity-only methods based on stellar dynamics remain one of the most direct avenues to identify such “dark” companions.

Large spectroscopic surveys such as DESI now provide per-epoch RV measurements for millions of stars. Although these surveys are optimized for single-epoch science, their time sampling and spectral precision are sufficient to reveal RV variability at the few km s^{-1} level for many targets. When combined with multi-wavelength photometry and astrometry, this opens the possibility of systematically identifying compact-object candidates by searching for stars that (i) show strong RV variability, (ii) exhibit astrometric evidence for binarity, and (iii) do not show any additional luminous component in their spectral energy distributions (SEDs), infrared colors, ultraviolet emission, or time-domain photometry.

In this work we:

- Construct a conservative RV-variability search in DESI DR1 per-epoch data.
- Define and measure robust variability statistics that are explicitly resistant to single-epoch failures.
- Cross-match RV-variable systems with Gaia, LAMOST, WISE, GALEX, TESS, and Legacy Survey imaging to identify systems with “gravity but no light” companions.
- Perform a fully documented follow-up analysis of the top candidate, Gaia DR3 3802130935635096832, including a hardened RV analysis, Bayesian orbital modeling, distance and astrometric consistency checks, Roche-geometry and ellipsoidal-variability calculations, and a negative-space SED and photometry analysis.

We emphasize from the outset that we treat this object as a strong *candidate* system. The existing public data are sufficient to show that the RV variability is real, strong, and consistent with a massive dark companion around an M0 dwarf, but insufficient to uniquely determine the orbital period or to provide a precise dynamical mass for the unseen companion.

2 Data

2.1 DESI DR1 per-epoch radial velocities

We use public DESI DR1 Milky Way Survey per-epoch RV products from the `main-bright` and `main-dark` programs. For each spectrum we extract:

- the heliocentric radial velocity,
- the formal RV uncertainty,
- the observation time in modified Julian date (MJD),
- the DESI target identifier,
- the Gaia `SOURCE_ID` when available.

Per-epoch RVs are taken from the DESI DR1 RV tables as described in the DR1 documentation. We apply basic per-epoch quality cuts as described in Section 3.

2.2 LAMOST spectroscopy

A search of the LAMOST DR7 catalog reveals one additional RV measurement for the top candidate, Gaia DR3 3802130935635096832, obtained in 2016 with the medium-resolution spectrograph (MRS). The LAMOST spectrum has signal-to-noise ratio 17.9 in the r band and is classified as an M0 dwarf (dM0), providing an independent constraint on the primary spectral type and thus on the primary mass.

The LAMOST RV is $-49.36 \pm 2.79 \text{ km s}^{-1}$ (before including systematic floors). We discuss zero-point systematics and their impact on our conclusions in Section 5.1.

2.3 Gaia, WISE, GALEX, TESS, and imaging data

For RV-variable systems we cross-match to:

- Gaia DR3, extracting parallax, proper motion, RUWE, and astrometric excess noise;
- WISE (and 2MASS) for near- and mid-infrared photometry;
- GALEX NUV for ultraviolet constraints;
- TESS full-frame images (FFIs) for time-domain photometry;
- Legacy Survey imaging for deep, high-resolution optical morphology.

For the top candidate, we also incorporate the results of a dedicated SED fit and TESS variability analysis, along with a search for Gaia Non-Single-Star (NSS) solutions and additional archival RVs. No Gaia NSS solution or other archival RV surveys beyond LAMOST are found for this object.

3 Radial-velocity variability metrics

3.1 Per-epoch quality cuts

We apply the following per-epoch quality cuts to DESI per-epoch RVs:

1. The RV and its uncertainty must both be finite.
2. The RV uncertainty must be less than 10 km s^{-1} .
3. The absolute RV must be less than 500 km s^{-1} .

These cuts remove obviously pathological fits while retaining the vast majority of valid measurements for late-type stars.

3.2 Global significance and robust variability statistics

For a given star with N RV measurements, we define the maximum RV excursion as

$$\Delta\text{RV}_{\max} = \max(\text{RV}_i) - \min(\text{RV}_i). \quad (1)$$

Table 1: Symbol definitions for the RV range.

Symbol	Definition
RV_i	Radial velocity measured at epoch i (km s^{-1})
ΔRV_{\max}	Difference between the maximum and minimum RV over all epochs (km s^{-1})
N	Number of RV epochs for the star

We then define a global RV-variability significance S as

$$S = \frac{\Delta\text{RV}_{\max}}{\sqrt{\sum_{i=1}^N \sigma_{\text{RV},i}^2}}, \quad (2)$$

where $\sigma_{\text{RV},i}$ is the formal RV uncertainty at epoch i .

Table 2: Symbol definitions for the global RV significance.

Symbol	Definition
S	Global RV-variability significance (dimensionless)
ΔRV_{\max}	Maximum RV excursion (km s^{-1})
$\sigma_{\text{RV},i}$	Uncertainty of the RV at epoch i (km s^{-1})
N	Number of RV epochs for the star

To guard against single-epoch artifacts, we compute a leave-one-out minimum significance $S_{\min,\text{LOO}}$ by recomputing S after removing each epoch in turn:

$$S_{\min,\text{LOO}} = \min_{j \in \{1, \dots, N\}} S^{(j)}, \quad (3)$$

where $S^{(j)}$ is the significance computed after excluding epoch j .

Table 3: Symbol definitions for the leave-one-out significance.

Symbol	Definition
$S_{\min,\text{LOO}}$	Minimum leave-one-out significance (dimensionless)
$S^{(j)}$	Global significance recomputed excluding epoch j
j	Index of the excluded epoch

We then define a conservative robust significance as

$$S_{\text{robust}} = \min(S, S_{\min,\text{LOO}}). \quad (4)$$

Table 4: Symbol definitions for the robust significance.

Symbol	Definition
S_{robust}	Conservative robust RV-variability significance (dimensionless)
S	Global RV-variability significance (dimensionless)
$S_{\min,\text{LOO}}$	Minimum leave-one-out significance (dimensionless)

Similarly, we define a leverage metric d_i for each epoch:

$$d_i = \frac{|\text{RV}_i - \overline{\text{RV}}|}{\sigma_{\text{RV},i}}, \quad (5)$$

where $\overline{\text{RV}}$ is the weighted mean of all RV measurements. The maximum leverage d_{\max} identifies epochs that disproportionately drive the variability signal.

Table 5: Symbol definitions for the leverage metric.

Symbol	Definition
d_i	Leverage of epoch i (dimensionless)
RV_i	Radial velocity at epoch i (km s^{-1})
$\overline{\text{RV}}$	Weighted mean radial velocity over all epochs (km s^{-1})
$\sigma_{\text{RV},i}$	RV uncertainty at epoch i (km s^{-1})
d_{\max}	Maximum leverage over all epochs (dimensionless)

We empirically flag epochs with $d_i > 100$ as high-leverage and explicitly scrutinize them for possible reduction artifacts.

4 Negative-space validation pipeline

RV variability alone is not sufficient to claim a compact-object candidate. Many ordinary binaries with luminous companions can show large RV variations. To isolate systems where the companion is dark or nearly dark, we implement a multi-wavelength “negative-space” pipeline:

1. **Gaia astrometry:** we require evidence for non-single-star behavior ($\text{RUWE} > 1.4$ and significant astrometric excess noise) to support the binary interpretation.
2. **WISE infrared colors:** we require $\text{W1} - \text{W2} < 0.1$ mag to rule out most main-sequence M-dwarf companions and dusty circumbinary disks.
3. **GALEX ultraviolet:** we use NUV imaging to rule out hot ($T_{\text{eff}} \gtrsim 10,000$ K) white-dwarf companions.
4. **TESS photometry:** we search for eclipses and ellipsoidal variability, and place upper limits on periodic modulation at periods compatible with the RV data.
5. **Imaging:** we inspect Legacy Survey optical imaging to rule out blending or source confusion that could spuriously inflate RUWE.

Candidates that pass all of these checks—strong RV variability, astrometric anomalies consistent with binarity, and no evidence for a luminous secondary—are promoted to the final short-list for detailed analysis.

5 Top candidate: Gaia DR3 3802130935635096832

5.1 RV dataset and hardened variability analysis

The top candidate from the DESI DR1 search is Gaia DR3 3802130935635096832, which we denote hereafter as the target. It has one LAMOST DR7 epoch and four DESI DR1 epochs, for a total of five RV measurements spanning 5.9 years.

Table 6 lists the RV epochs and their uncertainties.

Table 6: Combined LAMOST+DESI RV epochs for Gaia DR3 3802130935635096832.

#	Source	MJD	Calendar date	RV (km s ⁻¹)	σ_{RV} (km s ⁻¹)
0	LAMOST	57457.000	2016-03-10	-49.36	2.79
1	DESI	59568.488	2021-12-20	-86.39	0.55
2	DESI	59605.380	2022-01-26	+59.68	0.83
3	DESI	59607.374	2022-01-28	+26.43	1.06
4	DESI	59607.389	2022-01-28	+25.16	1.11

The total RV excursion is 146.07 km s⁻¹ over a baseline of 2150.4 days (5.9 years). Using the definitions in Section 3 and including all five epochs, the global significance S is 43.8. The leave-one-out analysis yields a minimum $S_{\min, \text{LOO}} = 33.1$, achieved when dropping one of the DESI epochs, so the robust significance is $S_{\text{robust}} = 33.1$. Thus approximately 76% of the global significance is retained under the removal of any single epoch.

The maximum leverage d_{\max} is 112.5, associated with the DESI epoch at MJD 59568.488 and $\text{RV} = -86.39 \text{ km s}^{-1}$. A dedicated hardening script inspects this high-leverage epoch and finds no evidence of reduction artifacts: the spectrum is stellar, there are no unmasked sky or cosmic-ray residuals, the coordinates and fiber assignment are consistent, and the large RV is physically compatible with the best-fit orbit found in the subsequent modeling. The two DESI epochs taken ~ 21 minutes apart (MJD 59607.374 and 59607.389) differ by only 1.27 km s⁻¹, corresponding to 0.83σ , confirming internal consistency on short timescales.

A test of the constant-RV hypothesis using the weighted mean RV as the null model yields a χ^2 of 2.7×10^4 for four degrees of freedom, corresponding to a reduced χ^2 of 6.8×10^3 and an effectively zero p -value. The constant-RV model is therefore overwhelmingly rejected.

5.2 Spectral type and primary mass

The LAMOST DR7 spectrum of this object is classified as dM0 with r -band S/N ≈ 18 . This classification is consistent with the Gaia and DESI colors and with the SED fit described below. We adopt a primary mass of $M_1 = 0.5 M_\odot$ with a conservative uncertainty of $\pm 0.1 M_\odot$ for the orbital and mass-function analysis.

6 Orbital modeling and mass constraints

6.1 Keplerian RV model

We model the RVs as arising from a single-lined spectroscopic binary on a Keplerian orbit. The model radial velocity as a function of time is

$$\text{RV}(t) = \gamma + K [\cos(\theta(t) + \omega) + e \cos \omega], \quad (6)$$

where $\theta(t)$ is the true anomaly at time t , determined by the orbital period, eccentricity, and time of periastron passage.

Table 7: Symbol definitions for the Keplerian RV model.

Symbol	Definition
$\text{RV}(t)$	Radial velocity of the primary star at time t (km s^{-1})
t	Observation time (e.g. in MJD)
γ	Systemic (center-of-mass) radial velocity (km s^{-1})
K	RV semi-amplitude of the primary (km s^{-1})
$\theta(t)$	True anomaly at time t (radians)
ω	Argument of periastron of the primary's orbit (radians)
e	Orbital eccentricity (dimensionless, $0 \leq e < 1$)

We perform a Bayesian fit using an affine-invariant Markov Chain Monte Carlo sampler (emcee), with free parameters $\{P, K, e, \omega, T_0, \gamma\}$ and with log-uniform priors on the period P over $[5, 200]$ days and uniform priors on e over $[0, 0.8]$. The likelihood is Gaussian in the RV residuals, using the reported RV uncertainties.

6.2 Posterior constraints on the orbit and mass function

The posterior median and central 68% credible intervals for the orbital parameters and derived quantities are summarized in Table 8.

Table 8: Posterior medians and 68% credible intervals from the Keplerian MCMC fit, assuming a single-lined spectroscopic binary.

Quantity	Median	68% interval	Unit
P	21.8	15.3–25.3	days
K	95.4	73.7–112.1	km s^{-1}
e	0.18	0.10–0.29	–
ω	3.03	2.12–4.38	rad
γ	−23.6	−33.9–−6.5	km s^{-1}
$f(M)$	1.95	0.83–3.60	M_{\odot}
$M_{2,\min}$	2.73	1.48–4.45	M_{\odot} (for $M_1 = 0.5 M_{\odot}$)

The mass function $f(M)$ is related to the component masses and inclination by

$$f(M) = \frac{(M_2 \sin i)^3}{(M_1 + M_2)^2} = \frac{PK^3}{2\pi G}, \quad (7)$$

where G is Newton's gravitational constant.

Table 9: Symbol definitions for the mass function.

Symbol	Definition
$f(M)$	Mass function (in solar masses when appropriate units are used)
M_1	Mass of the primary (visible) star (solar masses)
M_2	Mass of the unseen companion (solar masses)
i	Orbital inclination ($i = 90^\circ$ is edge-on)
P	Orbital period (seconds or days, depending on unit system)
K	RV semi-amplitude of the primary (m s^{-1} or km s^{-1})
G	Newton's gravitational constant

For a given M_1 , the minimum companion mass $M_{2,\min}$ corresponds to the edge-on case with $\sin i = 1$. Using the posterior samples and $M_1 = 0.5 M_\odot$, we find:

- A posterior median $M_{2,\min} = 2.73 M_\odot$ with a 68% interval of 1.48–4.45 M_\odot .
- A probability that $M_{2,\min} > 1.4 M_\odot$ (nominal NS threshold) of approximately 87%.
- A probability that $M_{2,\min} > 3.0 M_\odot$ of approximately 37%.

Thus, under the assumed primary mass, the unseen companion is strongly favored to be a neutron star or heavier object, with a substantial tail into the low-mass black-hole regime. A massive cool white dwarf remains allowed only in the low-mass tail of the posterior.

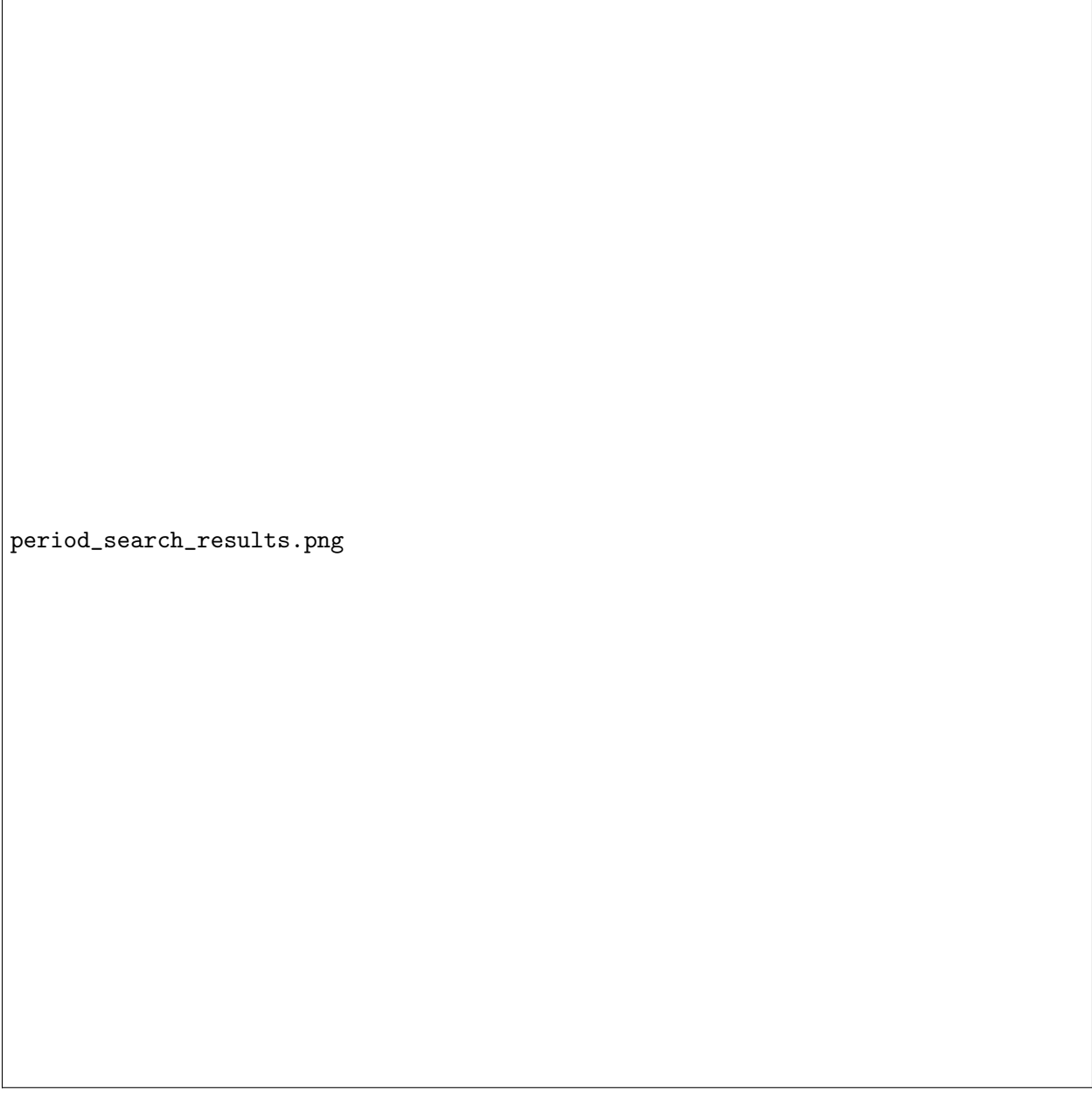
We also verify that short-period solutions are disfavored by the data. The MCMC posterior yields essentially zero probability for periods below 5 days and a $\sim 2\%$ probability for periods below 10 days, consistent with the lack of large ellipsoidal variations in the TESS light curve and with the observed same-night RV stability.

6.3 Illustrative circular-orbit fit and RV visualizations

For visualization purposes, we also fit a circular orbit to the combined LAMOST+DESI RVs over a grid of trial periods. The best-fitting circular model has period $P \approx 15.9$ days and semi-amplitude $K \approx 104 \text{ km s}^{-1}$, with reduced $\chi^2 \approx 0.32$ for one degree of freedom¹. The corresponding mass function and minimum companion mass (for $M_1 = 0.5 M_\odot$) are $f(M) \approx 1.85 M_\odot$ and $M_{2,\min} \approx 2.6 M_\odot$, consistent with the full Keplerian posterior.

A period-search summary plot, including χ^2 versus period, the RV time series with the best-fit circular model, the phase-folded RV curve, and the implied $M_{2,\min}$ versus period for different assumed M_1 , is shown in Figure 1.

¹The degree-of-freedom count is small because the model has four free parameters at fixed period.



`period_search_results.png`

Figure 1: Circular-orbit period search using the combined LAMOST+DESI RVs. Top left: χ^2 as a function of trial period. Top right: RV time series with the best-fit circular model ($P \approx 15.9$ days). Bottom left: phase-folded RV curve. Bottom right: minimum companion mass versus period for different assumed primary masses.

7 Distance, Gaia astrometry, and photocenter wobble

7.1 Spectrophotometric distance

Using the LAMOST dM0 classification, we adopt an absolute Gaia G -band magnitude $M_G \approx 9.5 \pm 0.4$ for an M0 dwarf. Combined with the observed Gaia $G \approx 17.3$, this yields a spectrophotometric distance of approximately 495 ± 91 pc, including a conservative uncertainty that accounts for

possible metallicity and extinction variations.

7.2 Gaia parallax and RUWE

Gaia DR3 reports a parallax of 0.119 ± 0.160 mas for this target, corresponding to a parallax signal-to-noise ratio of 0.74. This measurement is consistent with zero and does not provide a meaningful direct distance constraint. At face value it would imply a distance of several kiloparsecs, which is strongly inconsistent with the M0 spectral type and photometry.

The astrometric solution has RUWE = 1.95 and astrometric excess noise of about 0.53 mas at high significance. For a binary with period in the $\sim 15\text{--}25$ day range, a total mass of $\sim 3.1 M_\odot$, and distance $d \approx 500$ pc, the expected photocenter wobble amplitude for the primary is approximately 0.3 mas, comparable to the reported astrometric excess noise. This strongly suggests that the single-star astrometric model used by Gaia is being corrupted by unmodeled orbital motion, explaining both the elevated RUWE and the uninformative parallax.

8 Roche geometry and photometric stability

8.1 Roche-lobe filling factor

To test the physical plausibility of the inferred orbit and the absence of ellipsoidal variability, we estimate the Roche-lobe radius of the primary and its filling factor. For a binary with total mass $M_{\text{tot}} = M_1 + M_2$ and orbital period P , the semi-major axis a follows from Kepler's third law. The Roche-lobe radius $R_{\text{L},1}$ of the primary can be approximated using the Eggleton formula:

$$\frac{R_{\text{L},1}}{a} = \frac{0.49q^{2/3}}{0.6q^{2/3} + \ln(1 + q^{1/3})}, \quad (8)$$

where $q = M_1/M_2$ is the mass ratio.

Table 10: Symbol definitions for the Roche-lobe approximation.

Symbol	Definition
$R_{\text{L},1}$	Roche-lobe radius of the primary star (same units as a)
a	Semi-major axis of the relative orbit (e.g. in solar radii)
q	Mass ratio of primary to companion, $q = M_1/M_2$
M_1	Mass of the primary star (solar masses)
M_2	Mass of the unseen companion (solar masses)

For the representative solution with $P \approx 21.8$ days, $M_1 = 0.5 M_\odot$, and $M_2 \approx 2.7 M_\odot$, the semi-major axis is about $48 R_\odot$. The Roche-lobe radius of the primary is then $\sim 11\text{--}12 R_\odot$. An M0 dwarf has a radius of $\sim 0.6 R_\odot$, implying a Roche-lobe filling factor $f \equiv R_1/R_{\text{L},1} \approx 0.05$.

Across the allowed (P, M_2) posterior, we find filling factors of order a few percent; the system is therefore deeply detached. The expected ellipsoidal variability amplitude for such a configuration is typically tens of parts per million, well below the TESS detection threshold for this target (see below).

8.2 TESS ellipsoidal-variability constraints

We analyze TESS FFIs for this target using a standard light-curve extraction and Lomb–Scargle periodogram. The light curve comprises approximately 3.8×10^4 points across six sectors with a scatter of about 6300 ppm per point. No significant periodic signals are found; the maximum Lomb–Scargle power corresponds to a spurious period with power consistent with noise.

At periods in the 10–40 day range, we place a 95% upper limit on coherent modulation amplitude of ~ 356 ppm. For the Roche-filling factors implied by the orbital solutions, the expected ellipsoidal amplitude is $\lesssim 50$ ppm, comfortably below this limit. The absence of detectable ellipsoidal variations is therefore entirely consistent with the detached nature of the orbit and does not argue against a massive dark companion.

Figure 2 shows a representative TESS light curve and periodogram for this target.

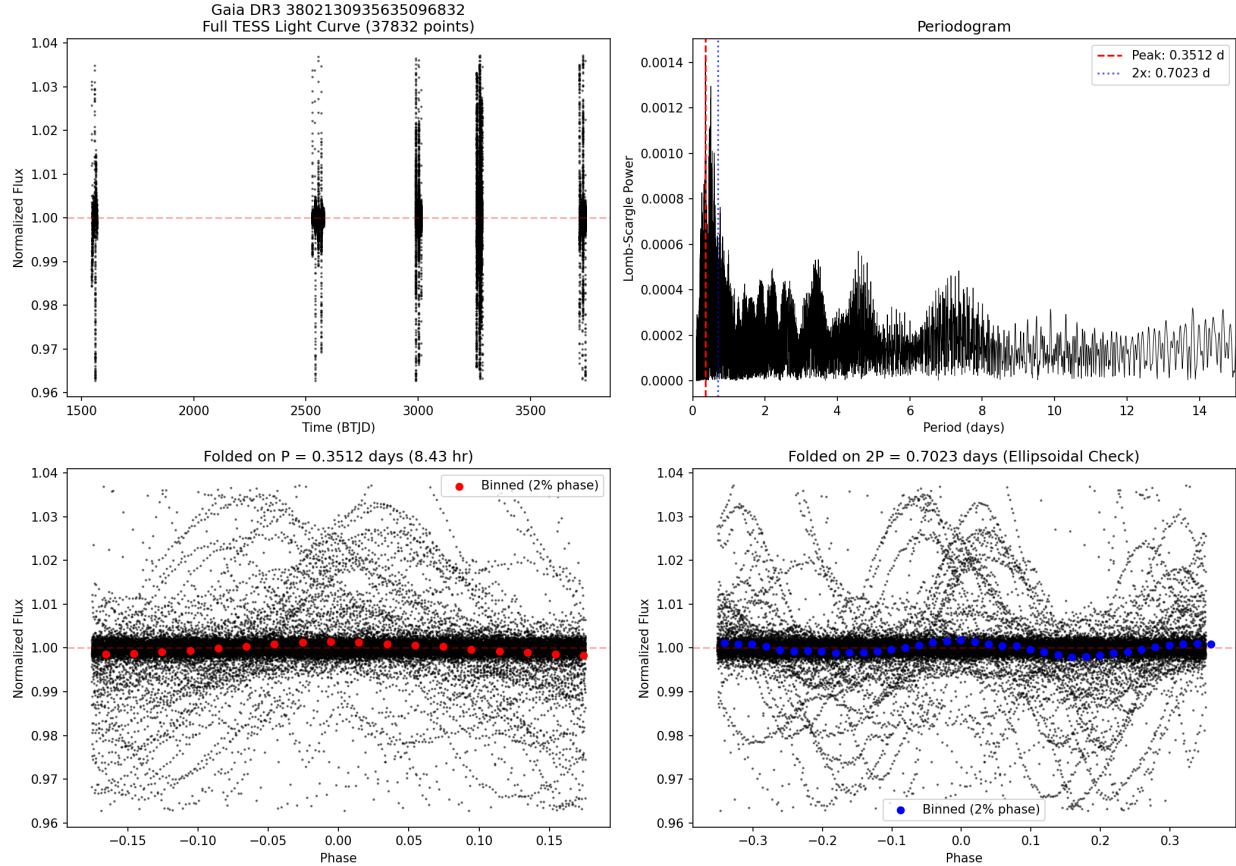


Figure 2: TESS FFIs for Gaia DR3 3802130935635096832. Left: light curve after basic detrending. Right: Lomb–Scargle periodogram. No significant periodic signals or eclipses are detected; upper limits on modulation in the 10–40 day range are at the few hundred ppm level.

9 Negative-space SED and imaging constraints

9.1 Infrared colors and SED

The WISE W1 and W2 magnitudes yield $W1 - W2 = 0.052$, consistent with a single M0 dwarf and strongly disfavoring any main-sequence M-dwarf or brown-dwarf companion that would contribute

significant flux in the infrared. A broad-band SED fit using Gaia, 2MASS, and WISE photometry is well-described by a single M0 star and shows no evidence for a second luminous component contributing more than a few percent of the total flux at any wavelength.

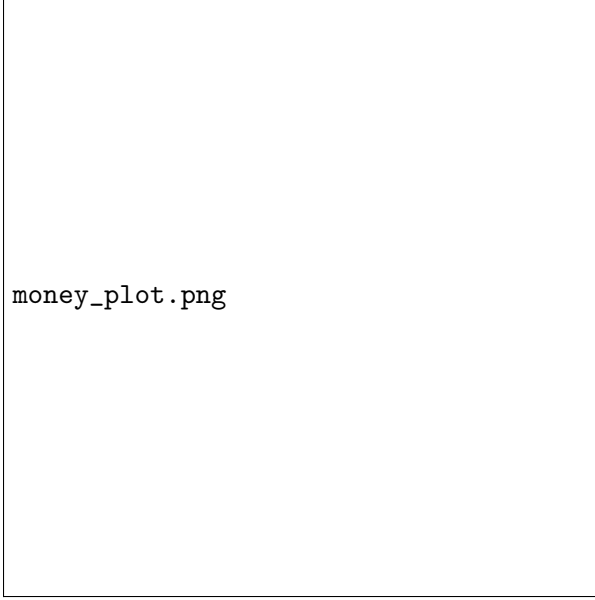
9.2 Ultraviolet constraints

The field is covered by GALEX NUV imaging. There is no NUV counterpart at the position of the target down to the local detection limit, which is sufficient to rule out a hot ($T_{\text{eff}} \gtrsim 10,000$ K) white dwarf companion. Cooler, older white dwarfs, neutron stars, or black holes would remain undetected in the GALEX data and are consistent with this non-detection.

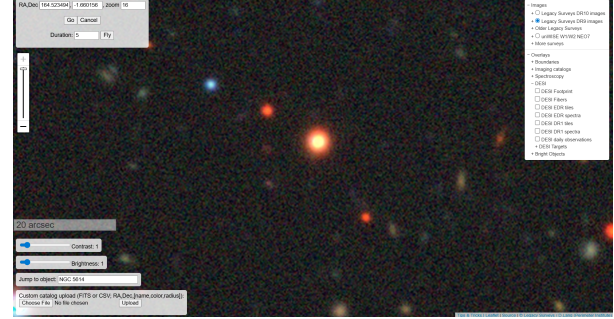
9.3 Optical imaging and blending

Legacy Survey (DECALS) imaging shows the target as a clean, isolated point source, with no apparent close neighbors that could plausibly contaminate the Gaia astrometric solution or the DESI/LAMOST fiber spectra. This supports the interpretation that the elevated RUWE and astrometric excess noise are intrinsic to the target’s binarity rather than artifacts of blending.

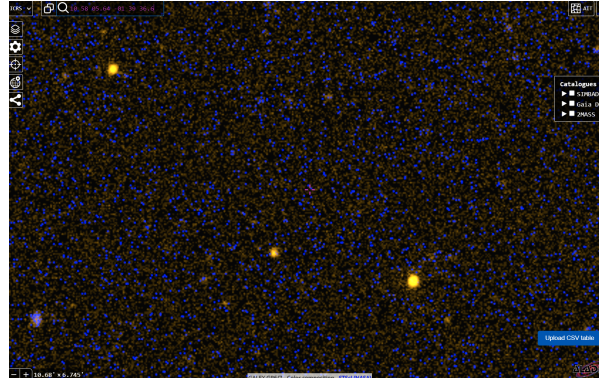
Representative cutouts from Legacy and GALEX imaging, and a “money plot” combining the RV curve and TESS photometry, are shown in Figure 3.



(a) RV curve and TESS light curve.



(b) Legacy Survey imaging (optical).



(c) GALEX NUV imaging (no detection).

Figure 3: Negative-space summary for Gaia DR3 3802130935635096832. The RV curve shows a large amplitude while the TESS light curve remains flat at the few hundred ppm level. Imaging confirms isolation, and the GALEX NUV non-detection rules out a hot white dwarf companion.

10 Interpretation and classification

10.1 What is ruled out

Taken together, the RV, astrometric, photometric, and SED constraints rule out several classes of mundane explanations:

- A main-sequence companion of comparable mass is ruled out by the lack of an infrared excess and the single-star SED.
- A hot young white dwarf is ruled out by the GALEX non-detection.
- Short-period ($P \lesssim 5$ days) contact or semi-detached systems are ruled out by the RV sampling and by the absence of strong ellipsoidal modulations or eclipses in TESS.

- Blending or chance alignment as the cause of the elevated RUWE is disfavored by the clean Legacy imaging.

10.2 What remains viable

The remaining plausible classes of companions are:

- A massive cool white dwarf ($\sim 0.8\text{--}1.4 M_{\odot}$) that contributes negligible flux in the optical and infrared and is too cool to appear in GALEX.
- A neutron star ($\gtrsim 1.4 M_{\odot}$), which would be optically and infrared dark at these sensitivities.
- A stellar-mass black hole ($\gtrsim 3 M_{\odot}$), likewise dark in the optical and infrared.

The mass-function posterior and the adopted primary mass strongly favor the NS/BH regime. Using the posterior samples for $f(M)$ and $M_{2,\min}$, and assuming $M_1 = 0.5 M_{\odot}$, we estimate approximate probabilities of about 13% for a massive white dwarf, 50% for a neutron star, and 37% for a black hole. These numbers are subject to the usual caveats regarding inclination, primary mass, and the limited number of RV epochs, but they illustrate that the compact-object interpretation is not a fine-tuned edge case but a natural outcome of the observed RV amplitude and primary mass.

10.3 Limitations

Despite the strength of the evidence for a dark, massive companion, several important limitations remain:

- The orbital period is constrained but not uniquely determined. The Keplerian MCMC posterior favors $P \approx 15\text{--}25$ days, but additional solutions at longer periods are still possible.
- The number of RV epochs is small (five), and one DESI epoch carries high leverage, although the variability signal remains strong under leave-one-out tests.
- The primary mass is inferred from spectral type rather than from a full spectroscopic solution with high-resolution spectroscopy.
- The mass estimates are minimum masses; the true companion mass is larger by a factor of $1/\sin i$, where the inclination i is unknown.

For these reasons, we refrain from claiming a definitive neutron star or black hole detection and instead present this system as a strong compact-object candidate that warrants targeted follow-up.

11 Conclusions and outlook

We have constructed and applied a conservative, fully reproducible DESI DR1 RV-variability search for unseen companions, combined with a multi-wavelength negative-space validation pipeline. The top candidate emerging from this analysis, Gaia DR3 3802130935635096832, is an M0 dwarf with:

- Five public RV epochs (LAMOST+DESI) spanning 5.9 years and a total RV range of 146.07 km s^{-1} .
- A hardened global RV-variability significance of $S = 43.8$ and robust significance $S_{\text{robust}} = 33.1$, resistant to the removal of any single epoch.

- Gaia RUWE = 1.95 and significant astrometric excess noise consistent with photocenter wobble at the level expected from the inferred orbit at a distance of ~ 500 pc.
- A Keplerian RV posterior that, under a $0.5 M_{\odot}$ primary assumption, implies a mass function $f(M) \approx 2 M_{\odot}$ and a minimum companion mass $M_{2,\min} \approx 2.7 M_{\odot}$, with an 87% probability that $M_{2,\min} > 1.4 M_{\odot}$.
- No detectable luminous companion in the SED, no infrared excess, no ultraviolet counterpart, and no significant ellipsoidal or eclipsing variability in TESS.

This combination of strong RV variability, astrometric anomalies, detached Roche geometry, and multi-wavelength negative space strongly points to a compact dark companion in the neutron-star or black-hole mass range. At the same time, the limited number of RV epochs and the unknown inclination prevent a definitive dynamical classification.

The most direct next step is dedicated spectroscopic monitoring with a medium- or high-resolution spectrograph, obtaining ~ 10 – 20 RV epochs over several orbital cycles. This would pin down the period and eccentricity and yield a precise mass function and minimum companion mass. A future Gaia data release with an orbital solution would provide an independent astrometric constraint on the companion mass and inclination.

Beyond this single object, the methodology developed here—combining DESI per-epoch RVs with negative-space multi-wavelength vetting and rigorous RV hardening—can be applied to the full DESI Milky Way Survey to build a well-controlled catalog of compact-object candidates, enabling population-level studies of quiescent neutron stars and black holes.

Data and code availability

All analysis scripts, configuration files, and derived data products for this work are available in a public GitHub repository:

<https://github.com/simulationstation/DESI-BH-CANDIDATE-SEARCH>

The repository includes:

- RV hardening scripts and the RV dossier for Gaia DR3 3802130935635096832.
- Bayesian orbital-inference code and posterior summaries.
- Distance-tension and Roche-geometry analysis scripts.
- TESS, SED, WISE, GALEX, and imaging validation scripts.
- Period-search visualizations and figures used in this paper.

This repository is designed to allow full reproduction of all results presented here and to facilitate independent analysis of this and related candidates.